

Finite Element Modelling of Finite Single and Double Quantum Wells

A Major Qualifying Project Report

Submitted to the Faculty

of the

WORCESTER POLYTECHNIC INSTITUTE

In partial fulfilment of the requirements for the

Degree of Bachelor of Science

in

Physics

by

Yuchen Wang

Date: January 2017

APPROVED:

Professor L. Ramdas Ram-Mohan, Major Project Adviser

Professor Padmanabhan K. Aravind, Major Project Adviser

Abstract

A system of two two-dimensional quantum dots is one of the simplest system used to study wavefunction localization. In general, the system is approximated by two finite quantum wells in the vicinity of each other. The wavefunction of such a system is hard to solve analytically; thus, a more precise numerical method is always in demand to give a better description of the system. This report discusses the finite element method (FEM), which is originally developed for mechanical engineering but extended to physics. This report also discusses using Fermi function to approximate discontinuous physical properties of the system. The validity of these methods is demonstrated with numerical data calculated under various approximations.

Acknowledgements

I would like to thank all that made the completion of this project possible:

My project advisor, Dr. L. Ramdas Ram-Mohan, for taking me into his lab, all of his time, encouragement, patience, and help.

Center of Computational NanoScience at WPI, for the computational resources used for the numerical work.

My project co-advisor, Dr. Padmanabhan K. Aravind, for his advice and guidance.

My lab colleague, Christopher Pierce, for his help in my computational work.

Contents

| | |
|---|-----------|
| Abstract | i |
| Acknowledgements | ii |
| Table of Contents | iii |
| List of Figures | iii |
| List of Tables | vii |
| 1 Introduction | 1 |
| 2 Variational Principles and Finite element Analysis | 2 |
| 3 Fermi Function in 2D | 5 |
| 4 Double Quantum Dots Interaction | 11 |
| 4.1 Double Square dots | 11 |
| 4.2 Double Circular dots | 14 |
| 5 Conclusion | 18 |
| A The figures of the wavefunctions | 19 |
| A.1 square dots | 19 |
| A.2 circular dots | 30 |

List of Figures

| | | |
|----|---|----|
| 1 | Comparison between a step function and a Fermi function. . . | 7 |
| 2 | Inverse of mass to effective mass ratio (m_*/m_e) distribution for the square inside a square calculation. | 9 |
| 3 | Potential function for the square inside a square calculation. . | 11 |
| 4 | Inverse of mass to effective mass ratio (m_*/m_e) distribution for the double square dots calculation. | 12 |
| 5 | Potential function for the double dots calculation. | 13 |
| 6 | State 1 wavefunction of the square quantum dots with distance 100Å between. | 19 |
| 7 | State 2 wavefunction of the square quantum dots with distance 100Å between. | 20 |
| 8 | State 3 wavefunction of the square quantum dots with distance 100Å between. | 20 |
| 9 | State 4 wavefunction of the square quantum dots with distance 100Å between. | 21 |
| 10 | State 1 wavefunction of the square quantum dots with distance 50Å between. | 22 |
| 11 | State 2 wavefunction of the square quantum dots with distance 50Å between. | 22 |
| 12 | State 3 wavefunction of the square quantum dots with distance 50Å between. | 23 |

| | | |
|----|---|----|
| 13 | State 4 wavefunction of the square quantum dots with distance 50Å between. | 23 |
| 14 | State 1 wavefunction of the square quantum dots with distance 20Å between. | 24 |
| 15 | State 2 wavefunction of the square quantum dots with distance 20Å between. | 24 |
| 16 | State 3 wavefunction of the square quantum dots with distance 20Å between. | 25 |
| 17 | State 4 wavefunction of the square quantum dots with distance 20Å between. | 25 |
| 18 | State 1 wavefunction of the square quantum dots with distance 10Å between. | 26 |
| 19 | State 2 wavefunction of the square quantum dots with distance 10Å between. | 26 |
| 20 | State 3 wavefunction of the square quantum dots with distance 10Å between. | 27 |
| 21 | State 4 wavefunction of the square quantum dots with distance 10Å between. | 27 |
| 22 | State 1 wavefunction of the square quantum dots with distance 5Å between. | 28 |
| 23 | State 2 wavefunction of the square quantum dots with distance 5Å between. | 28 |

| | | |
|----|--|----|
| 24 | State 3 wavefunction of the square quantum dots with distance 5Å between. | 29 |
| 25 | State 4 wavefunction of the square quantum dots with distance 5Å between. | 29 |
| 26 | State 1 wavefunction of the circular quantum dots with dis- tance 100Å between. | 30 |
| 27 | State 2 wavefunction of the circular quantum dots with dis- tance 100Å between. | 31 |
| 28 | State 3 wavefunction of the circular quantum dots with dis- tance 100Å between. | 31 |
| 29 | State 4 wavefunction of the circular quantum dots with dis- tance 100Å between. | 32 |
| 30 | State 1 wavefunction of the circular quantum dots with dis- tance 50Å between. | 33 |
| 31 | State 2 wavefunction of the circular quantum dots with dis- tance 50Å between. | 33 |
| 32 | State 3 wavefunction of double quantum dots with distance 50Å between. | 34 |
| 33 | State 4 wavefunction of the circular quantum dots with dis- tance 50Å between. | 34 |
| 34 | State 1 wavefunction of the circular quantum dots with dis- tance 2Å between. | 35 |

| | | |
|----|--|----|
| 35 | State 2 wavefunction of the circular quantum dots with distance 2\AA between. | 35 |
| 36 | State 3 wavefunction of the circular quantum dots with distance 2\AA between. | 36 |
| 37 | State 4 wavefunction of the circular quantum dots with distance 2\AA between. | 36 |

List of Tables

| | | |
|---|--|----|
| 1 | Eigenvalues obtained using different number of elements. . . . | 4 |
| 2 | Eigenvalues obtained using different interpolation polynomials. | 5 |
| 3 | Eigenvalues obtained using the Fermi function with various δ values | 10 |
| 4 | Eigenvalues of two square quantum dots with various distances in between. | 15 |
| 5 | Eigenvalues of two circular quantum dots with various distances in between. | 17 |

1 Introduction

In quantum mechanics, every system can be described by a Schrödinger's equation with appropriate potential terms. Due to complicated potential terms and boundary conditions (BCs), analytically solving Schrödinger's equation is hard in general. However, the variational principle provides a universal way to address this equation. The numerical results of the eigenfunctions corresponding to the wavefunction and the eigenvalues corresponding to energy can be obtained via the finite element method (FEM).

The system of two 2D quantum dots is treated in two cases: two square quantum wells and two circular quantum wells. Since different materials usually compose the inside and outside regions of the quantum dots, there is a discontinuity in the material properties across the boundary of the potential wells. This discontinuity will lead to difficulties in numerical analysis. Hence, an approximation is needed to resolve this problem. The report discusses the Fermi function as a smooth approximation of the discontinuity at the boundary.

In this report, Section II provides the methodology of the variational principle and the FEM. Section III discusses the validity of the Fermi function approximation. The numerical data of the wave functions and the energy eigenvalues of an electron inside 2D quantum dots are presented and discussed in Section IV. Section V provides the summation and conclusion remarks of this report. Appendix lists selected figures of the wave functions to illustrate

the localization of the wave functions between the two dots.

2 Variational Principles and Finite element Analysis

Most of the physical properties obey differential equations which can be derived from the principle of stationary action. For a non-relativistic particle moving in a region with potential energy $V(\mathbf{r})$, the time-independent Schrödinger equation is given by

$$-\frac{\hbar^2}{2m}\nabla^2\psi(\mathbf{r}) + V(\mathbf{r})\psi(\mathbf{r}) = E\psi(\mathbf{r}). \quad (1)$$

The Schrödinger equation can be obtained under the condition that the action

$$A = \int d^3r \left[\nabla\psi^*(\mathbf{r}) \left(-\frac{\hbar^2}{2m} \right) \nabla\psi(\mathbf{r}) + \psi^*(\mathbf{r})(V(\mathbf{r}) - E)\psi(\mathbf{r}) \right] \quad (2)$$

has an extremum. Here ψ and ψ^* (the complex conjugate of ψ) can be considered as two independent fields. One can vary the action integral A with respect to $\psi^*(\mathbf{r})$ and set the variation to 0,

$$\delta A = \delta\psi^* \frac{\delta A}{\delta\psi^*} = 0. \quad (3)$$

The wave functions for the resulting Schrödinger's equation can be obtained from the solutions of the equation (3). [2]

The numerical solutions of the equation (3) can be obtained using FEM. In FEM, the action integral is rewritten as the sum of the partitioned action on each element.

To do the action integral for each element, we implement a polynomial interpolation for the wavefunction as $\psi = \phi_i N_i$. Here, ϕ_i denotes the i^{th} nodal value and N_i denote the interpolation polynomial at that node. We then integrate the actions using the interpolated wave functions over the element and write the results in matrix form. Then we overlay the element matrix onto the global matrix of the actions. During this process, when a node is present in more than one elements, the matrix component of the nodes in all the element matrices are adding together to ensure the continuity of the action. In this way, the action integral can be written in the matrix form as,

$$A = \sum_{\alpha\beta}^{nelem} \langle \psi_\alpha | K_{\alpha\beta} | \psi_\beta \rangle - \epsilon \langle \psi_\alpha | M_{\alpha\beta} | \psi_\beta \rangle. \quad (4)$$

Here, α and β are indices that go from 1 to the total number of elements ($nelem$), and the K matrix contains the kinetic part of the wavefunction, and the M is the overlap matrix that contains the potential part; whereas ϵ is the total energy of the system. We can minimize equation (4) with respect to $\langle \psi_\alpha |$ and obtain the discretized version of the Schrödinger equation in matrix form. To solve this matrix is to do a generalized eigenvalue problem.

Table 1: The first 10 energy eigenvalues of the infinite square potential well of the size $600 \times 600 \text{ \AA}$ with different *number of elements*. The interpolation polynomials type used is quintic hermite

| State No. (n_x, n_y) | 60 Elements | 180 Elements | 360 Elements | 600 Elements | Exact Eigenvalue |
|-----------------------------|--------------------|--------------------|--------------------|--------------------|---------------------|
| (1,1) | 2.000 000 315 964 | 2.000 000 011 741 | 2.000 000 001 457 | 2.000 000 000 391 | 2 |
| (1,2) | 5.000 001 155 247 | 5.000 000 042 963 | 5.000 000 005 350 | 5.000 000 001 100 | 5 |
| (2,1) | 5.000 001 155 250 | 5.000 000 042 964 | 5.000 000 005 369 | 5.000 000 001 344 | 5 |
| (2,2) | 8.000 004 186 648 | 8.000 000 155 827 | 8.000 000 019 496 | 8.000 000 004 238 | 8 |
| (1,3) | 10.000 002 782 276 | 10.000 000 102 993 | 10.000 000 012 841 | 10.000 000 002 861 | 10 |
| (3,1) | 10.000 002 820 148 | 10.000 000 105 203 | 10.000 000 013 180 | 10.000 000 002 909 | 10 |
| (2,3) | 13.000 010 227 649 | 13.000 000 380 295 | 13.000 000 047 547 | 13.000 000 010 235 | 13 |
| (3,2) | 13.000 010 227 651 | 13.000 000 380 296 | 13.000 000 047 560 | 13.000 000 010 436 | 13 |
| (1,4) | 17.000 004 723 575 | 17.000 000 175 616 | 17.000 000 021 941 | 17.000 000 004 717 | 17 |
| (4,1) | 17.000 004 723 577 | 17.000 000 175 616 | 17.000 000 021 954 | 17.000 000 004 905 | 17 |

The energy of the equation is given by the eigenvalues of the matrix. The corresponding eigenvectors are composed of values of the wave function at each node. Using the interpolation polynomials with the nodal values, we can plot the wavefunction over the whole region.

In the FEM calculation, we can improve the accuracy of the results by adding more elements (*h*-refinement) and by using higher order interpolation polynomials (called *p*-refinement). By increasing the number of elements and decreasing the size of each element, we get a better approximation of the wavefunction and thus improve the reliability of the interpolation. When we are using higher order interpolation polynomials, in addition to the continuity of the functional values, the values of higher order derivatives are also taken into account, which provides more details about the function. Table 1 and Table 2 present the data from the calculation of an infinite 2D potential well with different number of elements and different kinds of interpolation

Table 2: The first 10 energy eigenvalues of infinite square potential well of the size $600 \times 600 \text{ \AA}$ with different *interpolation polynomials*. The number of elements along each direction is 30.

| State No. (n_x, n_y) | Linear | Quadratic | Cubic hermite | Quintic hermite | Exact Eigenvalue |
|-----------------------------|--------------------|--------------------|--------------------|--------------------|---------------------|
| (1,1) | 2.002 072 976 968 | 2.000 000 809 195 | 2.000 009 490 588 | 2.000 002 514 726 | 2 |
| (1,2) | 5.023 403 002 383 | 5.000 018 656 386 | 5.000 036 310 359 | 5.000 009 185 818 | 5 |
| (2,1) | 5.023 403 002 383 | 5.000 018 656 386 | 5.000 036 310 360 | 5.000 009 185 819 | 5 |
| (2,2) | 8.044 733 027 798 | 8.000 036 503 577 | 8.000 138 421 374 | 8.000 033 253 701 | 8 |
| (1,3) | 10.090 019 505 074 | 10.000 278 643 245 | 10.000 080 984 889 | 10.000 022 309 353 | 10 |
| (3,1) | 10.090 019 505 074 | 10.000 278 643 246 | 10.000 093 282 900 | 10.000 022 343 845 | 10 |
| (2,3) | 13.111 349 530 489 | 13.000 296 490 437 | 13.000 331 225 894 | 13.000 081 457 404 | 13 |
| (3,2) | 13.111 349 530 489 | 13.000 296 490 437 | 13.000 331 225 894 | 13.000 081 457 404 | 13 |
| (1,4) | 17.339 273 291 118 | 17.001 264 311 523 | 17.000 162 669 871 | 17.000 037 609 686 | 17 |
| (4,1) | 17.339 273 291 118 | 17.001 264 311 524 | 17.000 162 669 871 | 17.000 037 609 687 | 17 |

polynomials. It can be shown that when we use quintic Hermite polynomial with 600 elements along each side, we can get results with double precision.

3 Fermi Function in 2D

The regions outside and inside of a quantum dot are composed of different materials, each of them with a different effective mass for the carrier and potential band-gap.[1] At the boundary of the two materials, there will be a discontinuity in these properties. This discontinuity will cause problems in FEM calculation when using Hermite interpolation, in which the continuity of the derivative of the function is taken into account. When using Hermite interpolation, we impose the continuity condition at the boundary of the elements by overlying parts from different local matrices that correspond to the same node. If we have a discontinuity at the boundary, the derivative

at the same node calculated from the two adjacent elements is different by a constant. We need to adjust this by multiplying the derivative nodal value of one of the elements by that constant so that the corresponding matrix value in both elements match up. It is hard to perform this for a complicated BCs because there is no simple algorithm to pick up all the adjacent element matrices at the boundary. Resolving this problem requires approximations that smooth out those discontinuous steps. The Fermi function, which originated in statistical physics to describe the Fermi-Dirac Distribution provides a good approximation for this condition. To show this graphically, we take an example of a 1D three-layer system with different effective mass in each layers. If m_r represents the ratio m_e/m^* , m_r along the region can be written as a Fermi function. The Fermi function provides an adjustable smoothing of the jump discontinuity at the boundary. Thus m_r is given by

$$m_r(x) = m_{ro} + \frac{m_{ri} - m_{ro}}{1 + \exp\left(\frac{(x-x_1)(x-x_2)}{\delta^2}\right)}. \quad (5)$$

Here, x_1 and x_2 are the coordinates of the two boundaries, δ is the parameter used to control the sharpness of the Fermi curve at the edge, m_{ri} is the value of $m_r(x)$ in the middle, and m_{ro} is the value of $m_r(x)$ on the two sides. A set of plots that corresponds to this set up is shown as FIG. 1.

From FIG. 1. it is clear that if the parameter δ is small enough, the Fermi function will quickly become horizontal when moving away from the boundary. The parameter δ can be used to control the fitness of the Fermi

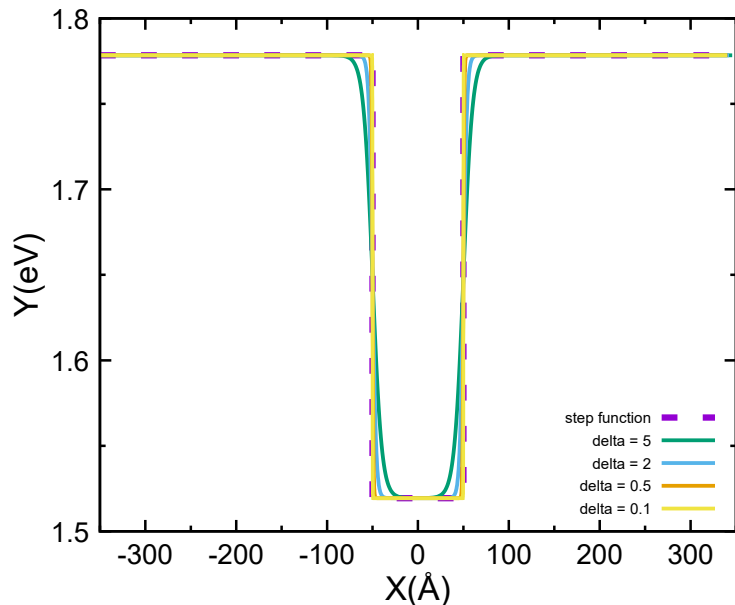


Figure 1: Comparison between a step function and a Fermi function.

function to the step function. It can be shown by doing quick math that a smaller δ value will give better fitness of the function. To give an example of the results using the Fermi function, Table 3 shows the calculations for a finite square inside a square potential well, where the Fermi function (take potential for example) is set up as

$$V(x) = V_{out} - \frac{V_{out} - V_{in}}{(1 + \exp(\frac{(x-x_1)(x-x_2)}{\delta^2})) (1 + \exp(\frac{(y-y_1)(y-y_2)}{\delta^2}))}. \quad (6)$$

In this equation, x_1 and y_1 are the smaller bound and x_2 and y_2 are the larger bound of the square region inside. This Fermi function will ensure the potential equals V_{in} inside the square region and V_{in} in the surrounding outer

square. FIG. 2 shows the effective mass distribution in the physical region in terms of mass ratio. FIG. 3 shows the potential function in the region. The shape of the function in these two figures are described by the Fermi function to provide a continuous approximation of the property difference across the boundary. Table ?? shows the results of the first ten eigenvalues obtained from this problem with various δ values. The potential band gap and effective mass ratio come from the heavy hole band width of AlGaAs and GaAs. The potential inside is $0eV$ and the potential outside is $0.159eV$. The ratio of electron mass to its effective mass inside is 2.86 and the ratio outside is 2.638. From the variational method in quantum mechanics, we know that the approximated results will always give an upper bound for the real value. From Table 3, when δ is smaller the results are smaller. So our data shows that for smaller δ values we get better results. It is also worth noticing that when δ is getting smaller the change in the resulting number is getting less significant. However, due to the limited capacity of the computer program, results will not be valid when using a extremely small δ value.

When we use the Fermi function to approximate the discontinuous properties at the boundary, We need to assign more elements in the adjacent of the boundary. This is because the graph of the Fermi is turning to vertical line very fast at the boundary, as shown in FIG. 1. To interpolation this behaviour properly, the size of the elements close to the boundary needs to be small. Applying more elements near the boundary can shrink the element size so that within each element the change in the function value is small

and can be represented properly by the interpolation polynomials. In order to have more elements at the boundary and try to reduce the overall number of elements, we can set up several intervals, each with different element density. The length of the intervals are given in terms of δ . We then assign more elements in the interval close to the boundary and assign a few elements to interval away from the boundary. This way we can represent the discontinuous properly at the boundary without using too much elements.

To summarize, using the Fermi function to approximate the step- function-like behaviour will give good numerical results when we assign more elements in the adjacent of the boundary and a small enough δ value.

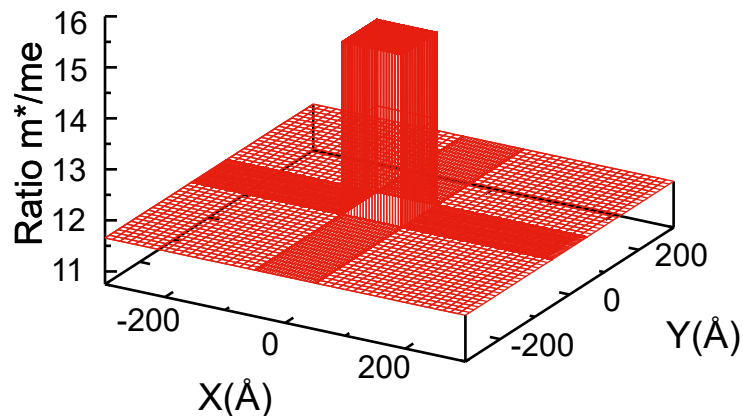


Figure 2: Inverse of mass to effective mass ratio (m_*/m_e) distribution for the square inside a square calculation.

Table 3: The first 10 energy eigenvalues of a finite potential square inside an infinite square potential well with various δ values. The size of the region is $600 \times 600 \text{ \AA}$ and the size of the finite well inside is $100 \times 100 \text{ \AA}$. Around the boundary there are three intervals. The sizes of these intervals 5, 5, 10 in terms of $\delta \text{ \AA}$ and the number of elements inside each interval are correspondingly 25, 10, 5. The total number of elements along each direction is 310. The effective mass and potential difference of the inside square and the outside square come from the heavy hole band gap of AlGaAs and GaAs. Parameter used in the calculation are further elaborated on in the text.

| Energy Eigenstates | $\delta = 0.5$ $10^{-3}eV$ | $\delta = 0.1$ $10^{-3}eV$ | $\delta = 0.05$ $10^{-3}eV$ | $\delta = 0.01$ $10^{-3}eV$ |
|--------------------|-------------------------------|-------------------------------|--------------------------------|--------------------------------|
| 1 | 15.599 597 506 491 | 15.599 587 280 724 | 15.599 586 560 589 | 15.599 586 003 793 |
| 2 | 38.758 694 071 697 | 38.758 672 070 459 | 38.758 670 538 591 | 38.758 669 354 742 |
| 3 | 38.758 694 071 733 | 38.758 672 070 763 | 38.758 670 539 295 | 38.758 669 361 244 |
| 4 | 61.733 240 851 152 | 61.733 207 910 490 | 61.733 205 627 558 | 61.733 203 882 489 |
| 5 | 76.357 094 213 602 | 76.357 063 911 059 | 76.357 061 868 547 | 76.357 060 311 942 |
| 6 | 76.560 231 572 882 | 76.560 200 073 149 | 76.560 197 941 915 | 76.560 196 290 390 |
| 7 | 99.028 297 790 542 | 99.028 257 598 005 | 99.028 254 876 732 | 99.028 252 810 697 |
| 8 | 99.028 297 790 641 | 99.028 257 598 609 | 99.028 254 877 917 | 99.028 252 820 181 |
| 9 | 126.155 187 366 676 | 126.155 163 516 181 | 126.155 162 034 658 | 126.155 160 894 802 |
| 10 | 126.155 187 366 819 | 126.155 163 517 511 | 126.155 162 037 583 | 126.155 160 920 987 |

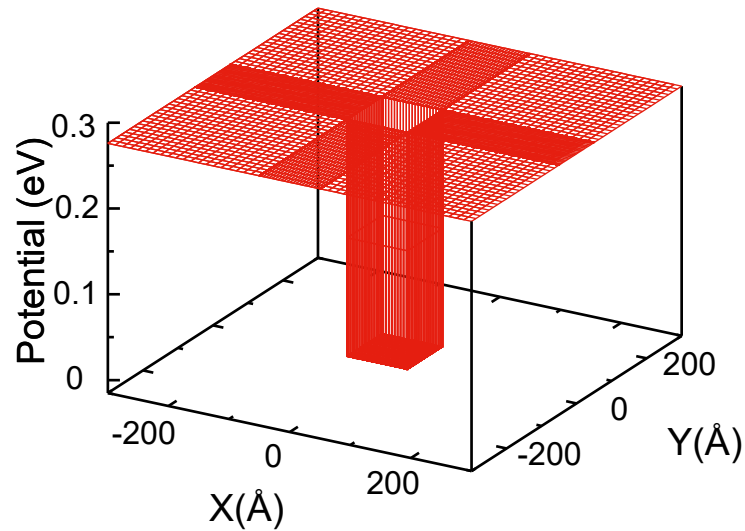


Figure 3: Potential function for the square inside a square calculation.

4 Double Quantum Dots Interaction

In a 2D region where there are two separated quantum dots, a particle can tunnel through the barrier between the dots if the dots are close enough to each other. The localization of the wavefunction inside two dots and the shift of the energy eigenvalue are discussed in this section.

4.1 Double Square dots

The quantum dots here are two squares that each have the width of 200\AA . They are symmetric to each other about the central y -axis. The distance between them is allowed to vary, and its effect to the wavefunction and eigenvalue is calculated. Outside the two dots, the width of surrounded region is set to 300\AA to allow the wavefunction to die out properly at the outside

boundary. The Fermi function that is used to describe the discontinuous properties at the dots boundary is

$$P(x) = P_{out} - \frac{P_{out} - P_{in}}{(1 + \exp(\frac{(x-x_1)(x-x_2)}{\delta^2})) (1 + \exp(\frac{(y-y_1)(y-y_2)}{\delta^2}))} - \frac{P_{out} - P_{in}}{(1 + \exp(\frac{(x-x_3)(x-x_4)}{\delta^2})) (1 + \exp(\frac{(y-y_1)(y-y_2)}{\delta^2}))}, \quad (7)$$

where P denotes the properties such as effective mass or potential, and x_1 and x_2 , y_1 and y_2 are the boundary coordinates of the first dot and x_3 and x_4 , y_1 and y_2 are the boundary coordinates of the second dot. The effective mass distribution and the potential function are shown in FIG. 4 and FIG. 5 respectively.

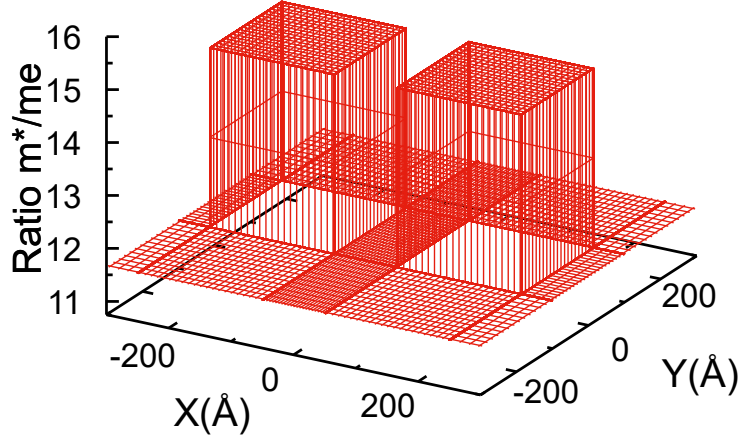


Figure 4: Inverse of mass to effective mass ratio (m_*/m_e) distribution for the double square dots calculation.

Table 4 shows the energy eigenvalues of each calculation with different separation distance. It is clear that when the distance in between is wide

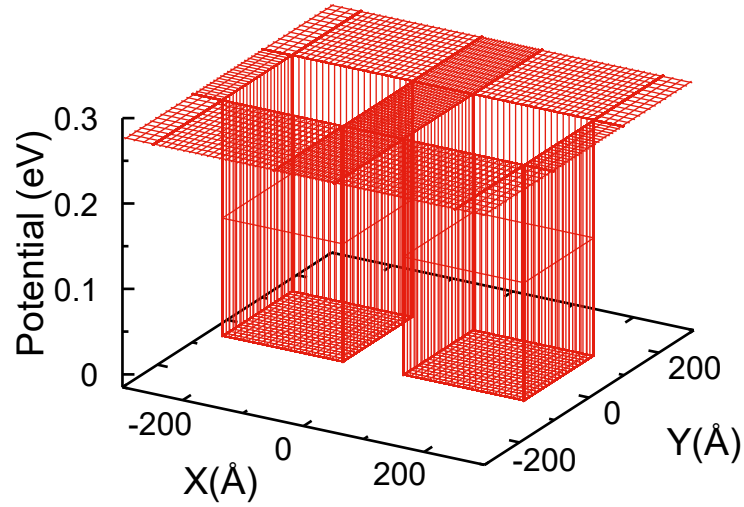


Figure 5: Potential function for the double dots calculation.

enough for both wavefunctions to die out within the barrier, there is a two-fold degeneracy of each state. This is due to the symmetry in the shape of the two dots. When two dots are moving towards each other, the degeneracy is broken up due to the possibility of particle tunneling through the barrier. From the data, when the distance in between is shrinking, some of the states are moving upward while others are moving downward and no state remains the same. When the two dots are close enough, the energy of the lower states may surpass the energy of the originally higher states. It can also be shown from the data that when the distance is changing in one direction, the change of energy is strictly in one direction. In another word, when a state's energy is increasing, it is strictly increasing while the distance is decreasing. Similarly, when a state's energy is decreasing, it is strictly decreasing while the distance is decreasing. The next section shows the figures to the wavefunctions of the

first few states with square dots. The merging of the two waves is clearly shown when the two dots are getting closer to each other.

4.2 Double Circular dots

The quantum dots in this set of calculation are two squares with a radius of 100\AA . The center of the two dots is on the same horizontal line. The physical region around the two dots is a rectangle with the dimension $1600\text{\AA} * 800\text{\AA}$. The distance between the dots is set to be the distance between the two center subtract two times the radius. This distance is allowed to vary, and its effect to the wavefunction and eigenvalue is calculated. The changing of the potential energy and effective mass at the circular boundary is described by a Fermi function

$$P = P_{out} - \frac{P_{out} - P_{in}}{1 + \exp(\frac{r_1 - r}{\delta})} - \frac{P_{out} - P_{in}}{1 + \exp(\frac{r_2 - r}{\delta})}. \quad (8)$$

P is the physical property the function is used to described. r is the radius of the circle and r_1 and r_2 is the distance of the point of interest to the two center.

Table 5 shows the first 10 energy eigenvalues of each calculation with different separation distance. From the comparison of circular dots and square dots, there are two things worth noticing. Firstly, the energy eigenvalues are changed in different geometry. This is because the first ten states are all bound states whose energy is lower than the potential energy of the finite

Table 4: The first 10 energy eigenvalues of two square quantum dots with various distances in between. The region around the two dots has a width of 300\AA and the size of each quantum dots is $200 \times 200\text{\AA}$. The distant between the two dots is label at the first row. Around the boundary of each dots there are three intervals. The sizes of these intervals are 5, 10, 15 in terms of δ and the number of elements inside each interval are correspondingly 20, 5, 5. The total number of elements is 500×260 . The effective mass and potential difference of the quantum dots and outside regions come from the conduction band gap of AlGaAs and GaAs.

| Energy States | 600 \AA 10^{-3}eV | 100 \AA 10^{-3}eV | 50 \AA 10^{-3}eV | 20 \AA 10^{-3}eV | 10 \AA 10^{-3}eV | 5 \AA 10^{-3}eV | 2 \AA 10^{-3}eV |
|---------------|--|--|---------------------------------------|---------------------------------------|---------------------------------------|--------------------------------------|--------------------------------------|
| 1 | 20.836 422 199 670 | 20.835 100 121 851 | 20.774 318 396 776 | 20.118 138 582 876 | 18.917 294 350 815 | 17.336 452 410 640 | 15.475 914 436 979 |
| 2 | 20.836 422 199 671 | 20.837 743 070 250 | 20.896 724 597 006 | 21.368 030 748 688 | 21.827 053 070 788 | 22.134 891 850 030 | 22.339 315 476 143 |
| 3 | 51.936 770 519 614 | 51.929 120 355 622 | 51.654 137 644 621 | 49.251 022 804 996 | 45.812 256 970 293 | 42.485 069 134 872 | 39.697 940 387 413 |
| 4 | 51.936 770 519 648 | 51.935 173 197 156 | 51.868 898 454 421 | 51.190 237 242 611 | 49.976 272 319 298 | 48.403 167 439 914 | 46.578 656 865 835 |
| 5 | 51.936 770 710 457 | 51.938 366 003 649 | 52.002 528 038 120 | 52.485 632 521 805 | 52.944 491 745 190 | 53.249 924 319 354 | 53.452 313 388 626 |
| 6 | 51.936 770 710 489 | 51.944 416 576 120 | 52.213 457 441 230 | 54.123 707 150 544 | 55.943 479 400 734 | 57.166 297 176 020 | 57.979 676 702 098 |
| 7 | 82.767 557 754 244 | 82.758 230 637 324 | 82.458 259 567 420 | 79.991 414 418 447 | 76.568 435 868 404 | 73.318 462 214 748 | 70.627 544 592 084 |
| 8 | 82.767 557 754 336 | 82.776 877 991 618 | 83.070 034 401 976 | 85.027 273 894 116 | 86.845 362 737 204 | 88.057 837 193 614 | 87.265 840 497 500 |
| 9 | 103.235 545 037 256 | 103.213 558 121 556 | 102.473 373 756 346 | 97.925 812 416 043 | 93.252 112 917 984 | 89.750 726 250 653 | 88.862 536 087 359 |
| 10 | 103.235 545 037 396 | 103.250 628 879 649 | 103.191 020 016 176 | 102.468 360 792 840 | 101.232 540 304 087 | 99.677 350 952 017 | 97.920 658 764 772 |

wells. Therefore the energy of the bound states should depend on the geometry and the size of the quantum well. Secondly, the degeneracy pattern is different and can be shown by looking at the last four states of dots that have distance 600\AA in between. In the square dots, there are two doublet degeneracies and the difference is quite significant, but in circular dots difference in all the four states are much less than that of square dots. The degeneracy pattern is determined by the symmetry of the system and can be predicted using group theory. The square and circle have different symmetry; therefore, the degeneracy pattern should be different. There are also many similarities between this two set of data. Firstly, it is clear that for the circular wells when the distance is large enough, there will be a doublet degeneracy of every state same as that of the square wells. When the two circle are getting closer to each other, the degeneracy is broken due to the possibility of electron tunneling through. Secondly, similar to that of the square, when the distance between the circle is decreasing, the change of energy of the same state is strictly in one direction. The next section also shows the figures to the wavefunctions of the first few states with circular dots. The merging of the two waves is clearly shown when the two dots are getting closer to each other.

Table 5: The first 10 energy eigenvalues of two circular quantum dots with various distances in between. The physical region around the two dots is a rectangle with the dimension $1600\text{\AA} * 800\text{\AA}$ and the radius of each quantum dots is 100\AA . The center of two circle is on the same horizontal line and the distant between the two dots is denoted at the first row. The node density (\AA per node) on the circle is 0.5. The node density on the outside is 40. The mesh is generated with Gmsh and the mesh element is triangle. The effective mass and potential difference of the quantum dots and outside regions come from the conduction band gap of AlGaAs and GaAs. The δ used for this calculation is 0.01\AA

| Energy States | 600\AA $10^{-3}eV$ | 100\AA $10^{-3}eV$ | 50\AA $10^{-3}eV$ | 2\AA $10^{-3}eV$ |
|---------------|--------------------------------|--------------------------------|-------------------------------|------------------------------|
| 1 | 24.301 762 | 24.299 946 | 24.271 749 | 22.520 824 |
| 2 | 24.301 848 | 24.301 157 | 24.328 896 | 25.174 874 |
| 3 | 61.479 926 | 61.469 889 | 61.307 540 | 54.336 396 |
| 4 | 61.480 161 | 61.474 289 | 61.465 212 | 61.066 178 |
| 5 | 61.480 645 | 61.474 724 | 61.483 734 | 61.796 655 |
| 6 | 61.480 810 | 61.479 178 | 61.638 951 | 65.436 480 |
| 7 | 109.788 008 | 109.752 326 | 109.440 862 | 100.310 885 |
| 8 | 109.788 361 | 109.762 897 | 109.686 299 | 107.291 977 |
| 9 | 109.791 326 | 109.768 343 | 109.844 395 | 111.672 180 |
| 10 | 109.791 652 | 109.778 437 | 110.080 558 | 114.466 675 |

5 Conclusion

This MQP project provides a finite element modelling of single and double quantum dots. It also shows how to use the Fermi function as a continuous approximation of discontinuous functions. All of this shows the power of FEM in calculating the energy eigenvalues and modelling the wavefunctions of 2D systems. This report also discusses the localization of the wavefunctions in two adjacent square and circular quantum dots. The results of which provides details about electrons tunnelling through the barrier between the dots.

A system of two two-dimensional quantum dots is one of the simplest system used to study wavefunction entanglement between two electrons. The wavefunction of two electrons inside the double quantum dots is strongly correlated with the wavefunction of a single electron. The results of this report could be extended into the study of two electrons interaction and the entanglement between them in quantum wells.

A The figures of the wavefunctions

A.1 square dots

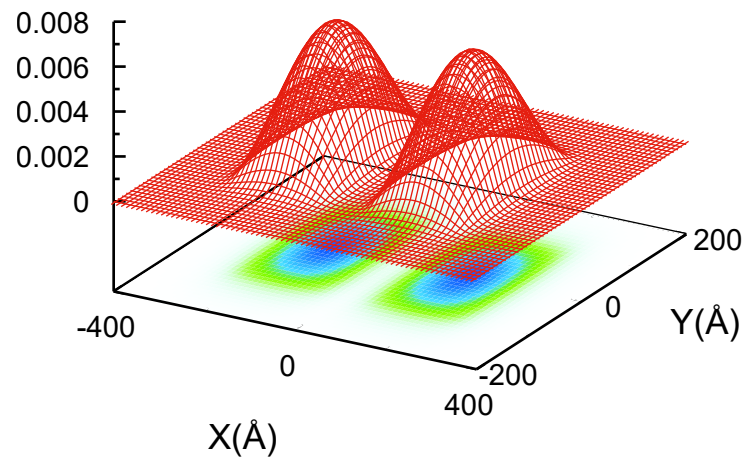


Figure 6: State 1 wavefunction of the square quantum dots with distance 100\AA between.

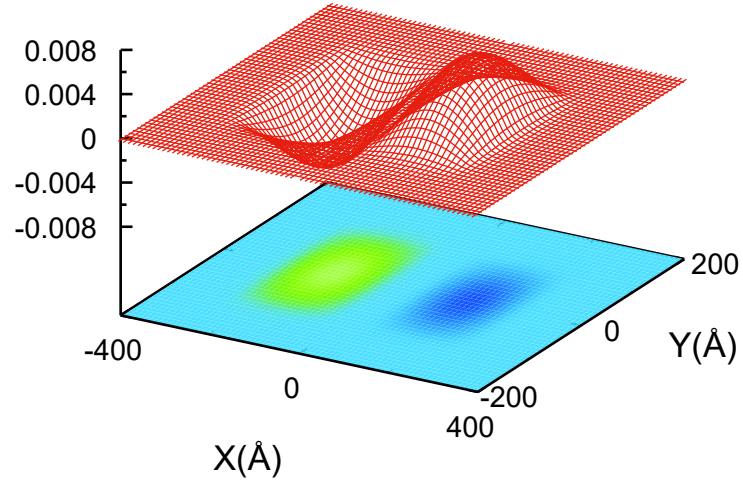


Figure 7: State 2 wavefunction of the square quantum dots with distance 100\AA between.

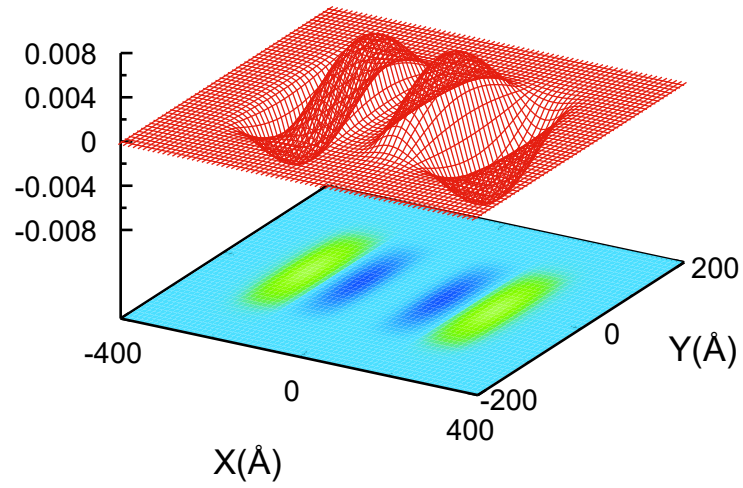


Figure 8: State 3 wavefunction of the square quantum dots with distance 100\AA between.

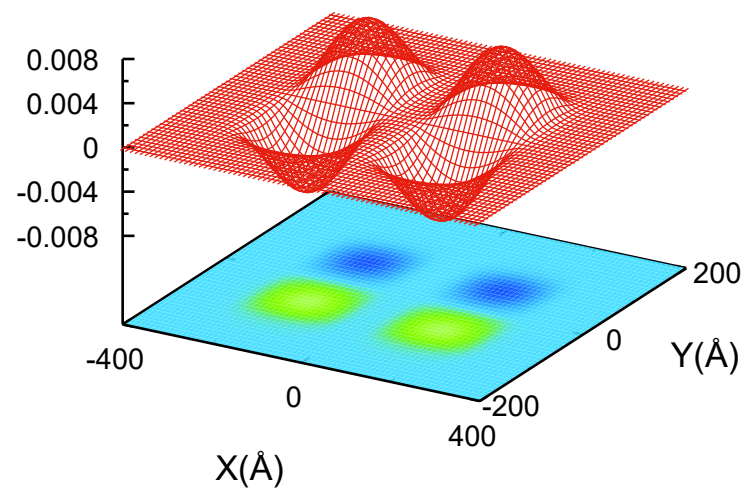


Figure 9: State 4 wavefunction of the square quantum dots with distance 100\AA between.

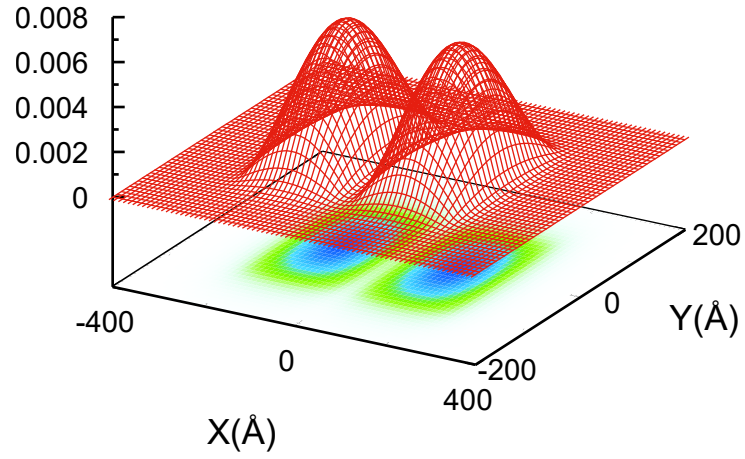


Figure 10: State 1 wavefunction of the square quantum dots with distance 50\AA between.

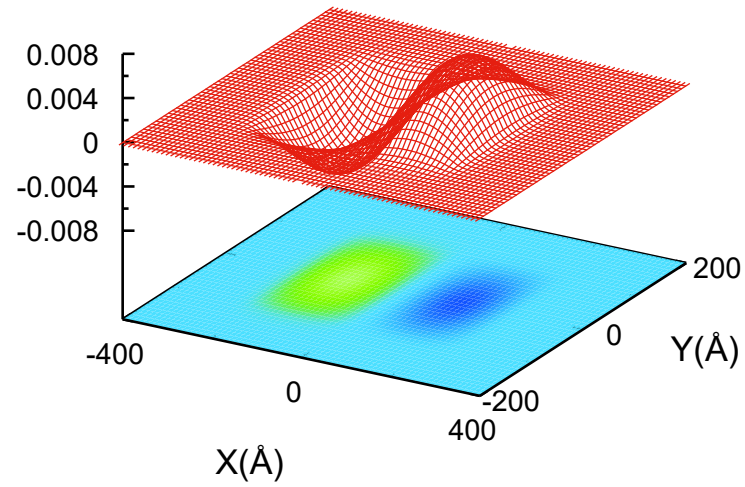


Figure 11: State 2 wavefunction of the square quantum dots with distance 50\AA between.

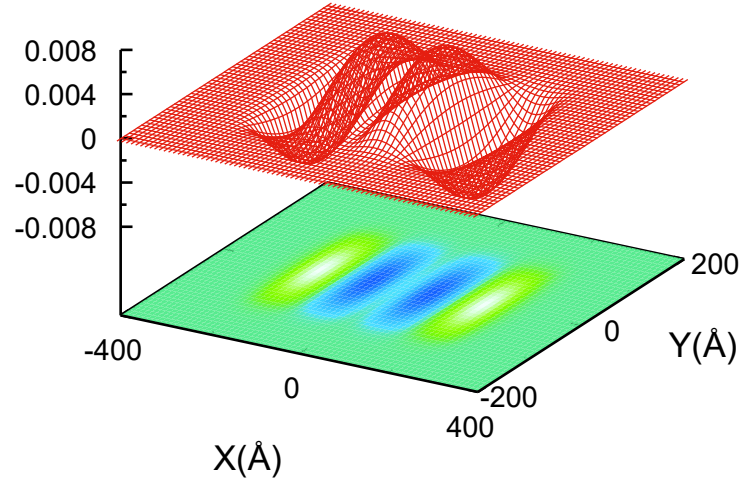


Figure 12: State 3 wavefunction of the square quantum dots with distance 50\AA between.

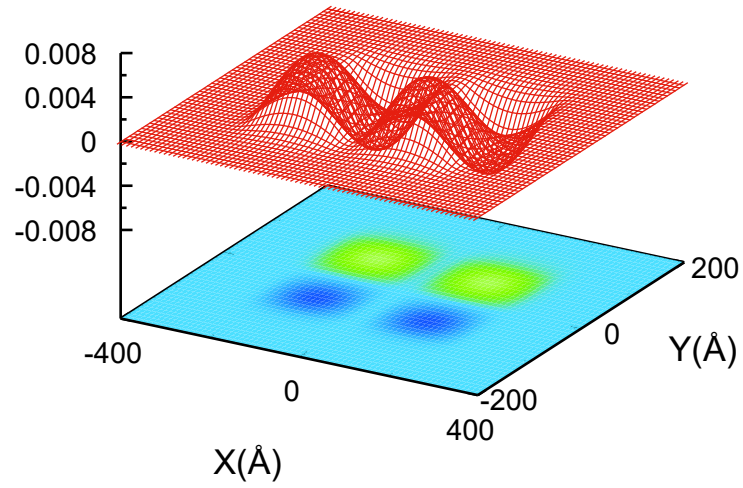


Figure 13: State 4 wavefunction of the square quantum dots with distance 50\AA between.

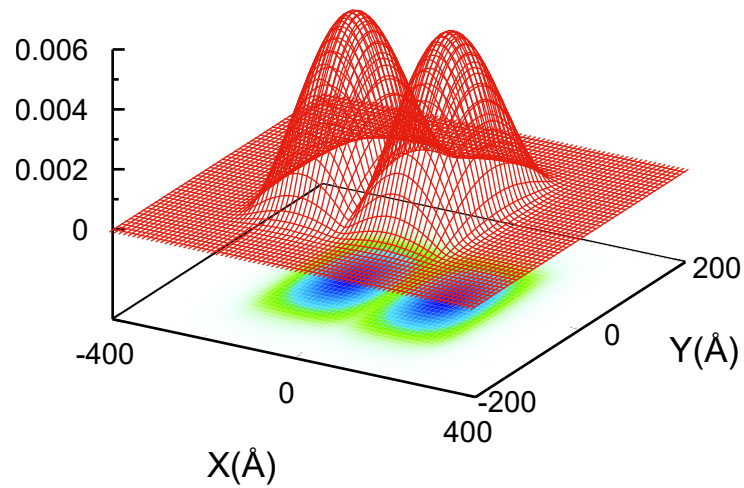


Figure 14: State 1 wavefunction of the square quantum dots with distance 20\AA between.

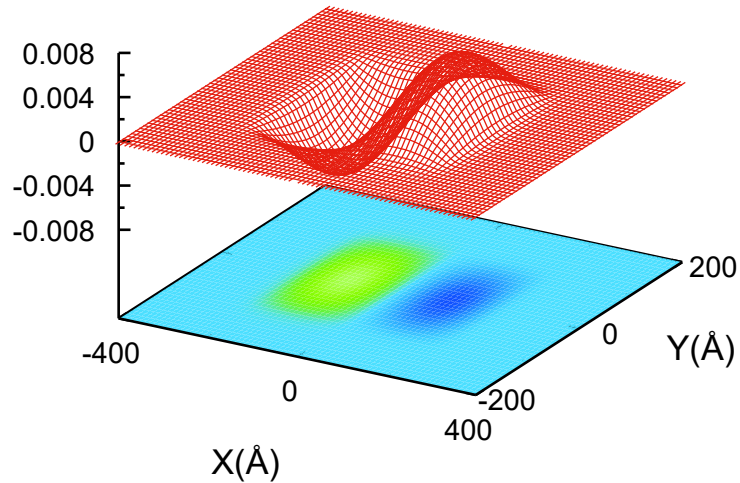


Figure 15: State 2 wavefunction of the square quantum dots with distance 20\AA between.

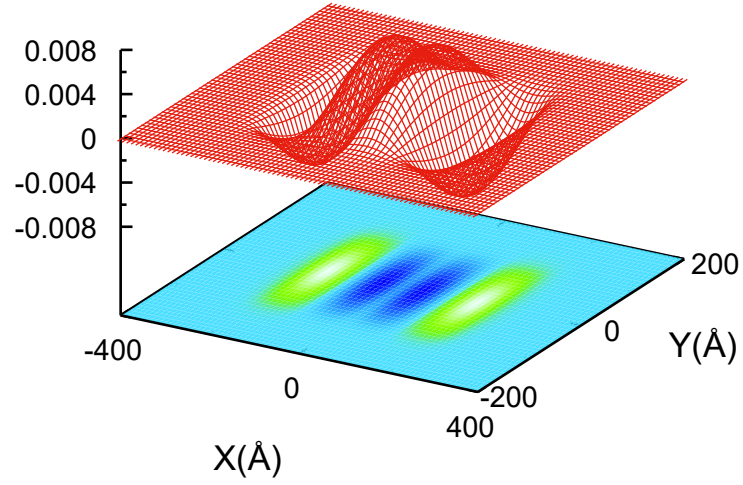


Figure 16: State 3 wavefunction of the square quantum dots with distance 20\AA between.

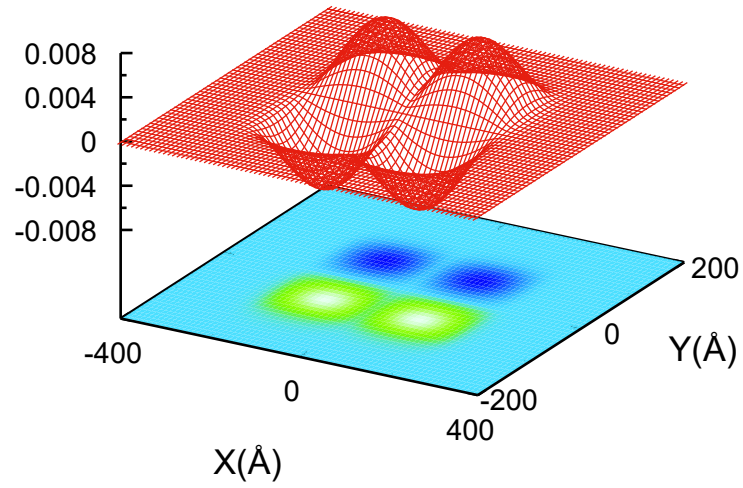


Figure 17: State 4 wavefunction of the square quantum dots with distance 20\AA between.

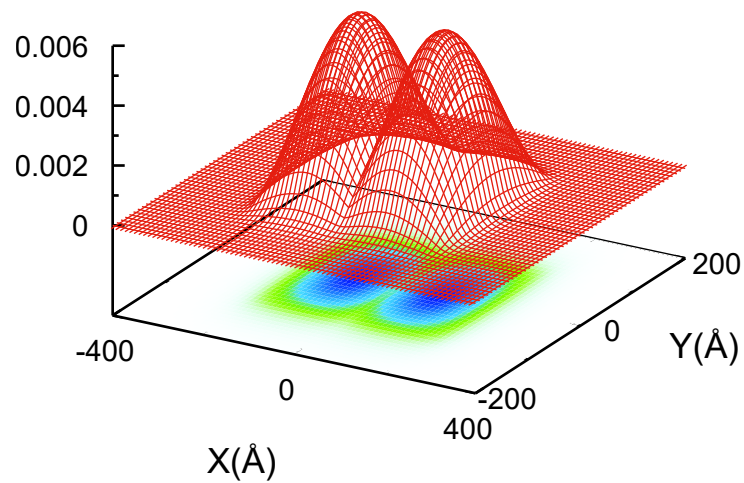


Figure 18: State 1 wavefunction of the square quantum dots with distance 10\AA between.

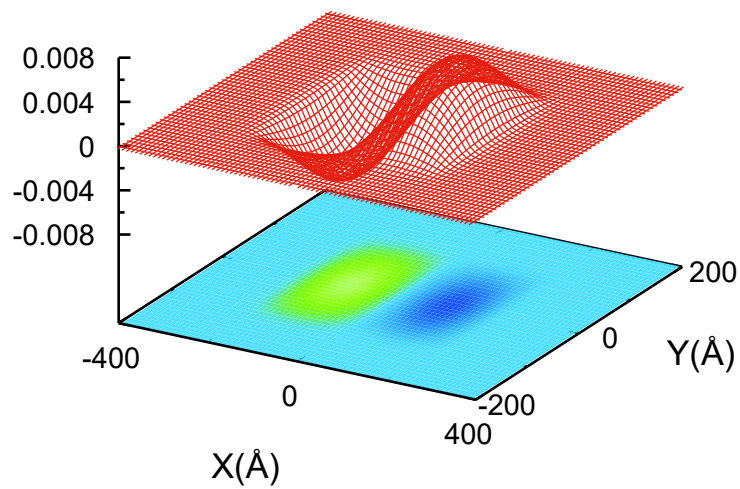


Figure 19: State 2 wavefunction of the square quantum dots with distance 10\AA between.

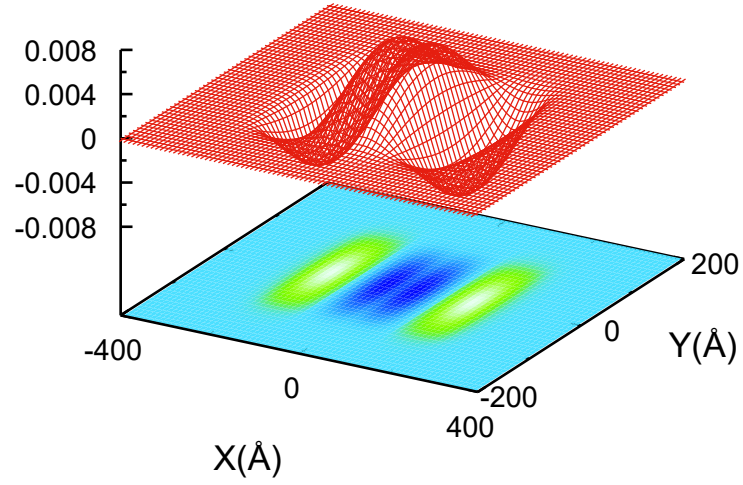


Figure 20: State 3 wavefunction of the square quantum dots with distance 10\AA between.

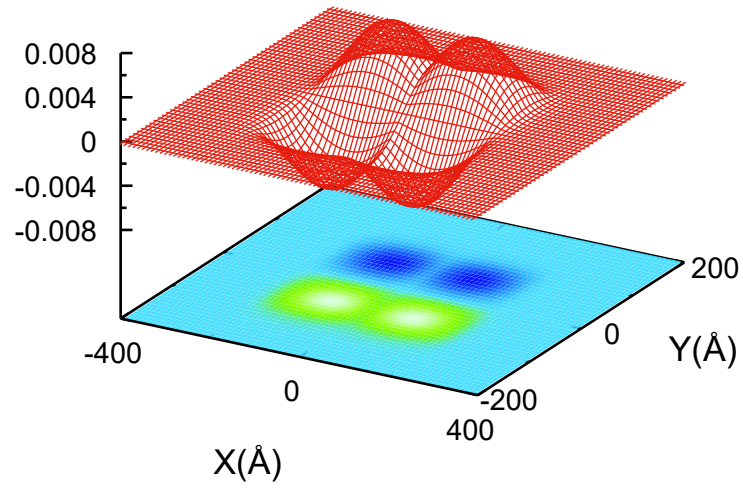


Figure 21: State 4 wavefunction of the square quantum dots with distance 10\AA between.

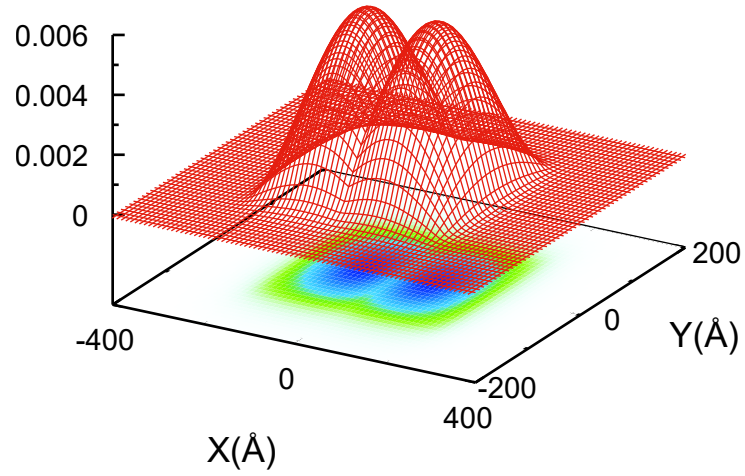


Figure 22: State 1 wavefunction of the square quantum dots with distance 5\AA between.

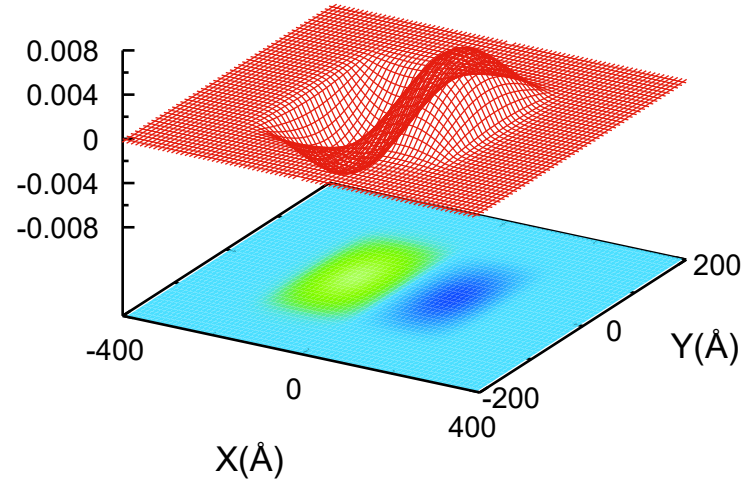


Figure 23: State 2 wavefunction of the square quantum dots with distance 5\AA between.

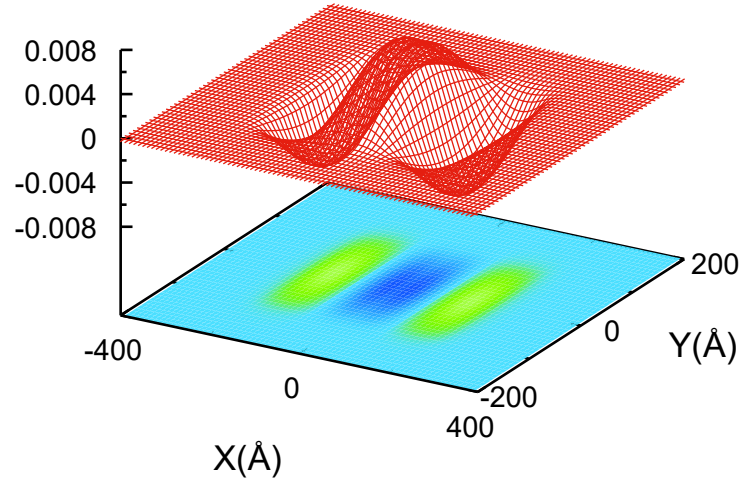


Figure 24: State 3 wavefunction of the square quantum dots with distance 5\AA between.

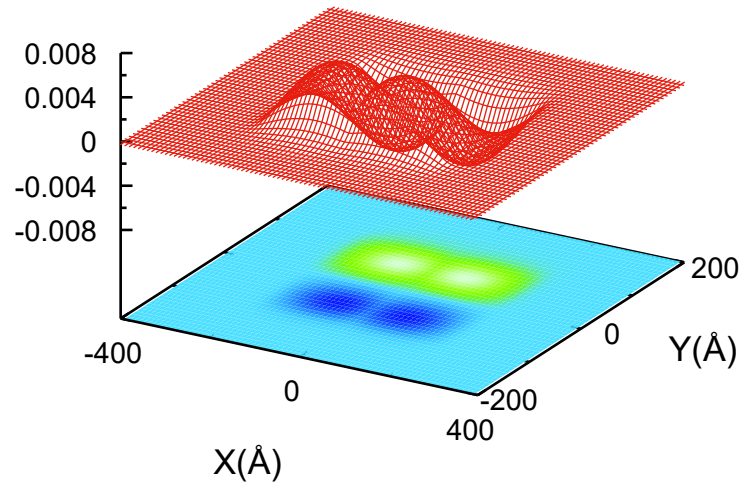


Figure 25: State 4 wavefunction of the square quantum dots with distance 5\AA between.

A.2 circular dots

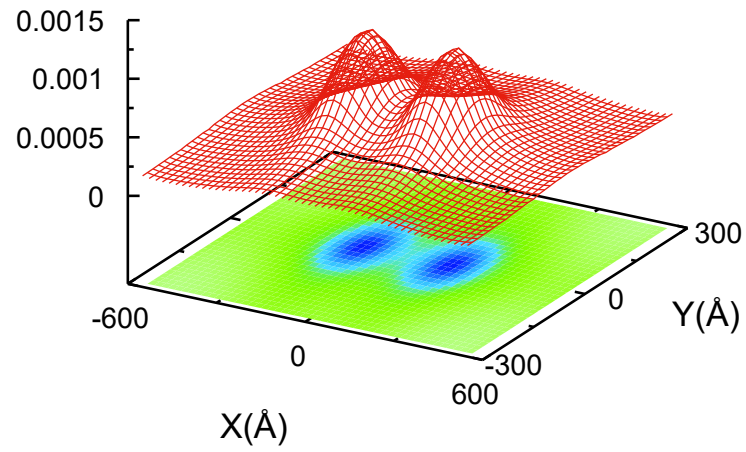


Figure 26: State 1 wavefunction of the circular quantum dots with distance 100\AA between.

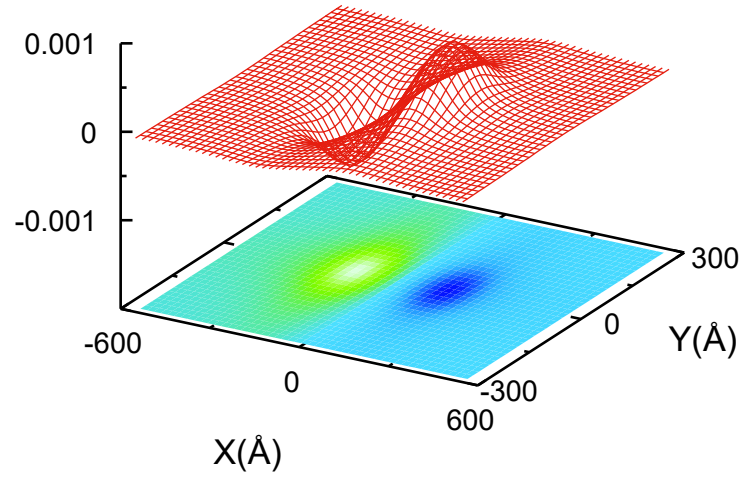


Figure 27: State 2 wavefunction of the circular quantum dots with distance 100\AA between.

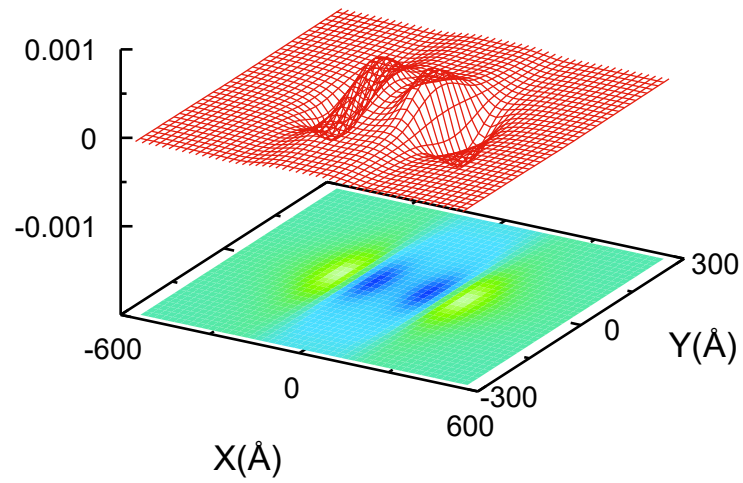


Figure 28: State 3 wavefunction of the circular quantum dots with distance 100\AA between.

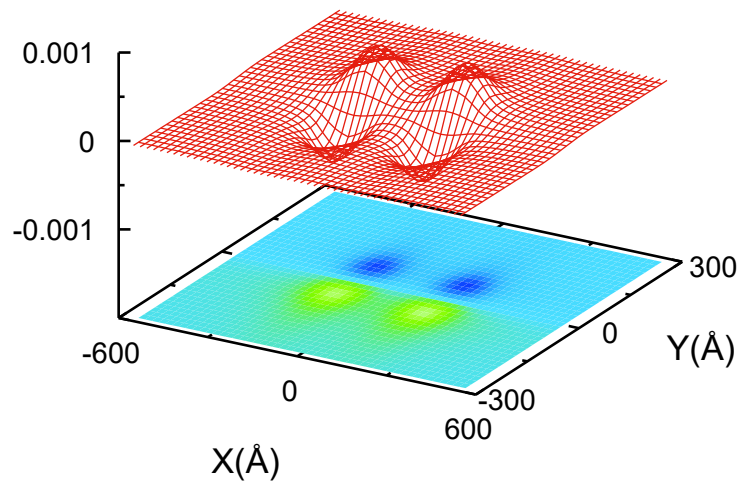


Figure 29: State 4 wavefunction of the circular quantum dots with distance 100\AA between.

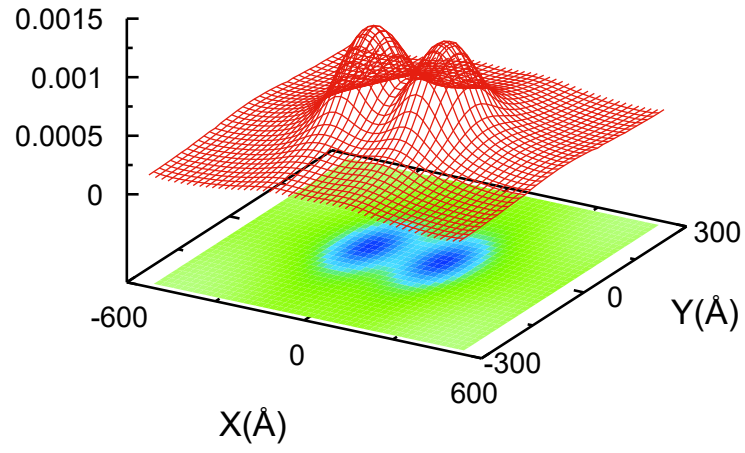


Figure 30: State 1 wavefunction of the circular quantum dots with distance 50\AA between.

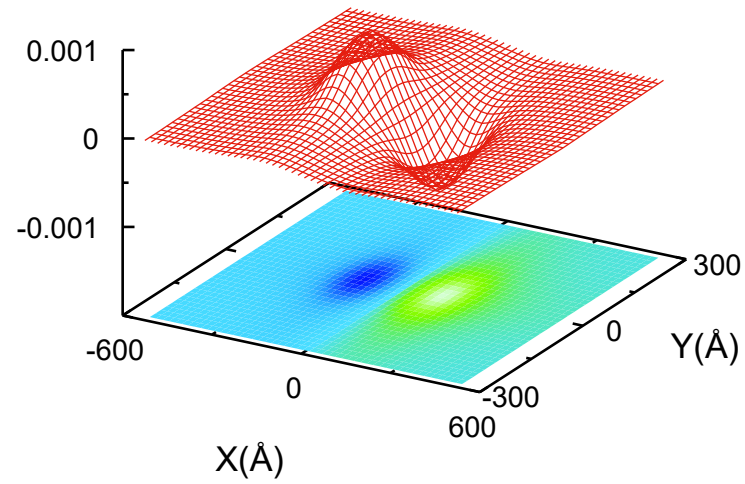


Figure 31: State 2 wavefunction of the circular quantum dots with distance 50\AA between.

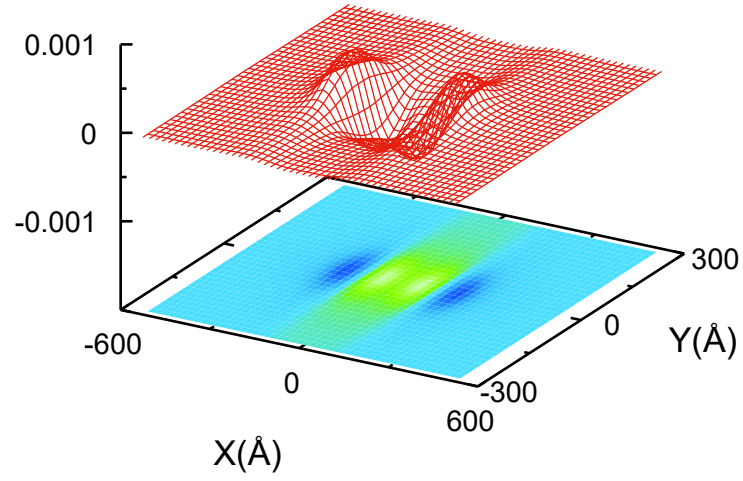


Figure 32: State 3 wavefunction of double quantum dots with distance 50\AA between.

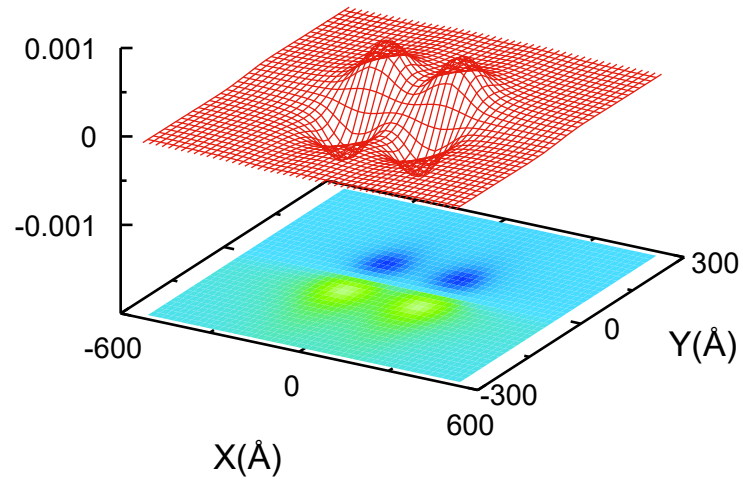


Figure 33: State 4 wavefunction of the circular quantum dots with distance 50\AA between.

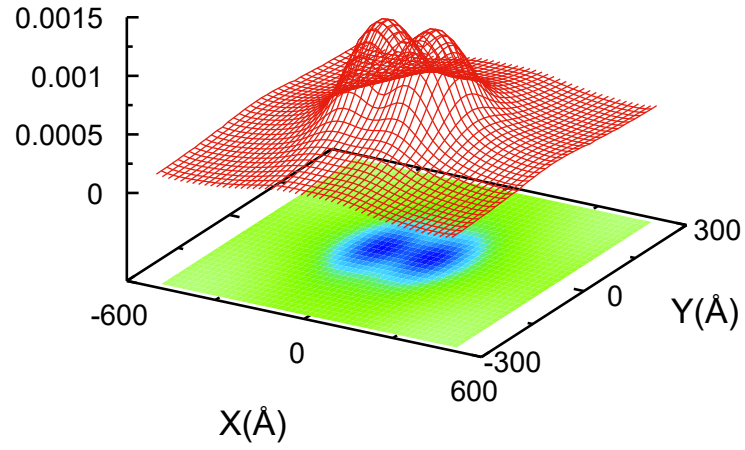


Figure 34: State 1 wavefunction of the circular quantum dots with distance 2\AA between.

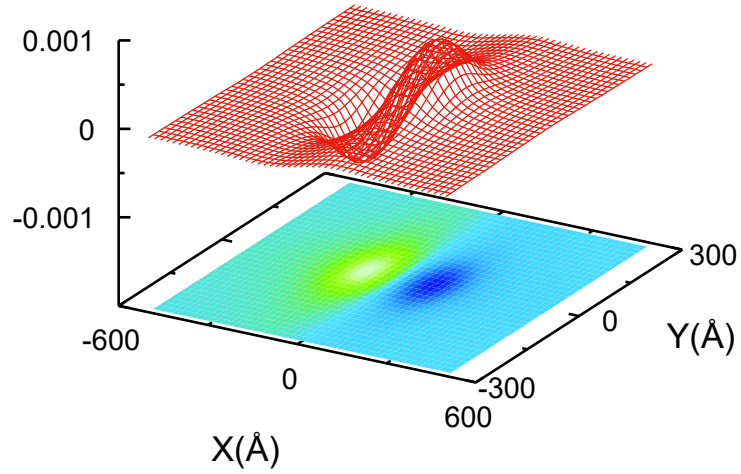


Figure 35: State 2 wavefunction of the circular quantum dots with distance 2\AA between.

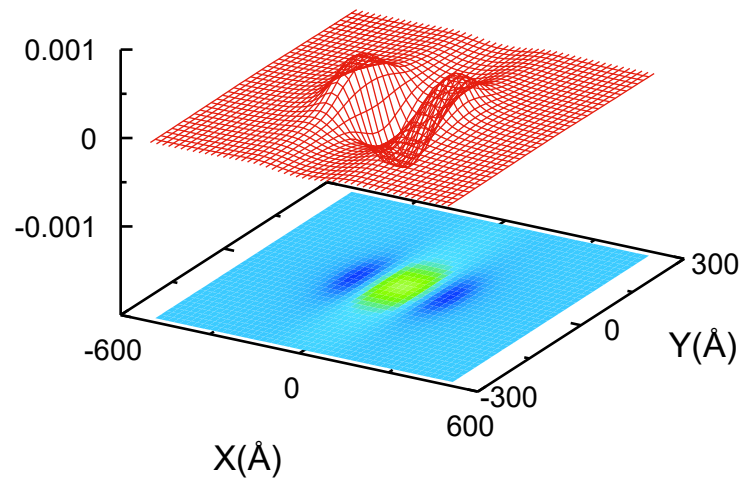


Figure 36: State 3 wavefunction of the circular quantum dots with distance 2\AA between.

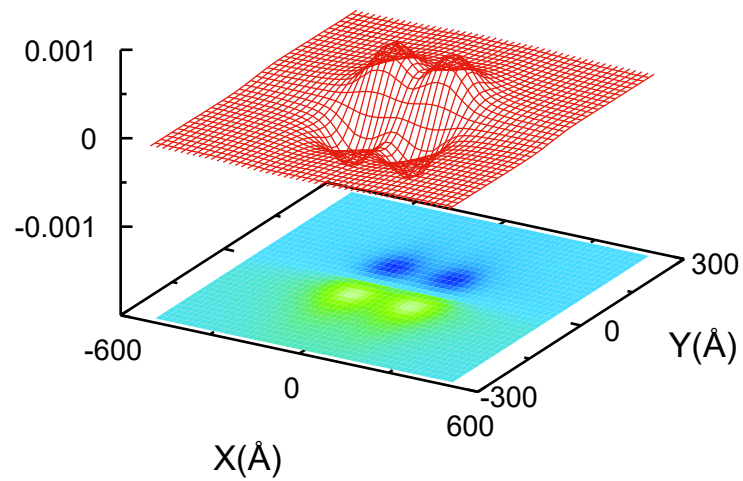


Figure 37: State 4 wavefunction of the circular quantum dots with distance 2\AA between.

References

- [1] Kittel, C., *Introduction to Solid State Physics* (John Wiley and Sons, Inc 2005).
- [2] L. R. Ram-Mohan, *Finite Element and Boundary Element Applications in Quantum Mechanics* (Oxford University Press, Oxford, 2002).